JOURNAL OF THERMOPHYSICS AND HEAT TRANSFER
Vol. 25, No. 2, April–June 2011

Entropy Generation in Non-Newtonian Fluids Along a Horizontal Plate in Porous Media

Waqar A. Khan*
National University of Sciences and Technology, Karachi 75350, Pakistan
and
Rama Subba Reddy Gorla†
Cleveland State University, Cleveland, Ohio 44114

DOI: 10.2514/1.51200

Second-law characteristics of heat transfer and fluid flow due to mixed convection of non-Newtonian fluids over a horizontal plate with a prescribed surface temperature in a porous medium are analyzed. Velocity and temperature fields are obtained numerically using an implicit finite difference method under the similarity assumption, and these results are used to compute the entropy generation rate *Ns*, the irreversibility ratio Φ, and the Bejan number *Be* for both pseudoplastic and dilatant fluids. The effects of the power-law index *n*, the temperature variation λ, the mixed convection parameter *γ*, the axial distance *x*, and the viscous frictional parameter *G* on the velocity and temperature profiles, the dimensionless entropy generation rate *Ns*, the irreversibility ratio Φ, and the Bejan number *Be* are investigated and presented graphically.

Introduction

EXERGY analysis relies on the laws of thermodynamics to establish the theoretical limit of ideal or reversible operation and the extent to which the operation of the given system departs from the ideal. The departure is measured by the calculated quantity called destroyed exergy or irreversibility. This quantity is proportional to the generated entropy. The minimization of entropy generation requires the use of more than thermodynamics; fluid mechanics, heat and mass transfer, materials, constraints, and geometry are also needed in order to establish the relationships between the physical configuration and the destruction of exergy. In the field of heat transfer, the entropy generation minimization method brings out the inherent competition between heat transfer and fluid flow irreversibilities in the optimization of devices subjected to overall constraints. Therefore, the main objective is to determine possible ways of minimizing it. The method used to achieve this purpose is known as entropy generation minimization or thermodynamic optimization. This method is used to analyze the irreversibilities present in real devices, concentrating special attention in finding the physical quantities that can be modified to optimize their specific performance.

Free and mixed convection boundary layers in Newtonian and non-Newtonian fluids over different geometries have been studied by several authors including [1–5]. The second-law analysis of a non-Newtonian fluid over a horizontal surface has many significant applications in thermal engineering and industries. Applications of horizontal surfaces can also be found in various industrial exchanger systems. One of the fundamental problems of the engineering processes is the improvement in thermal systems during the convection in any fluid. The second-law analysis is one of the best tools for improving the performance of the engineering processes. It investigates the irreversibility due to fluid flow and heat transfer in terms of the entropy generation rate. Bejan [6–8] employed this method in many convection problems and, later on, several other investigators used this method successfully in different heat transfer problems.

Saouli and Aiboud-Saouli [9] performed the second-law analysis for the Newtonian fluids along an inclined heated plate, whereas Saouli and Aiboud-Saouli [10] and Gorla and Pratt [11] performed the same analysis for non-Newtonian fluids with and without viscous dissipation effects. They considered the upper surface of the liquid film free and adiabatic and the lower wall fixed with constant heat flux. Their results show that the entropy generation number and the irreversibility ratio decrease in the transverse direction and increase as the viscous dissipation parameter increases. Recently, Aiboud-Saouli et al. [12] investigated the entropy generation in a laminar gravity-driven conducting liquid film along an inclined heated plate in the presence of a transverse magnetic field.

In this study, we investigated the second-law analysis of heat transfer and fluid flow due to mixed convection of non-Newtonian fluids over a horizontal plate with a prescribed surface temperature. The velocity and temperature distributions are determined by solving the Darcy's and energy equations, subject to an appropriate set of boundary conditions. The dimensionless entropy generation rate, irreversibility ratio, and the Bejan number were computed using numerical values of velocity, temperature, and their gradients. The dimensionless parameters governing the problem are the dimensionless temperature variation parameter, the fluid behavior index, the dimensionless transverse and axial distances, and the Peclet number.

Problem Formulation

Consider a steady mixed convection of a power-law fluid along an impermeable horizontal plate (Fig. 1) with a prescribed wall temperature ($\bar{T}_w = \bar{T}_\infty + A\bar{x}^\lambda$, where A and λ are specified constants) embedded in a porous medium. The isothermal surface conditions are represented by $\lambda = 0$. Nonisothermal surface conditions are represented by the power-law form for many practical applications. It is assumed that the physical properties of the power-law fluids, except the density, are constant and that the Boussinesq approximation for the case of maximum density is valid. The ambient temperature is $\bar{T}_\infty$, as shown in Fig. 1, where $\bar{x}$ and $\bar{y}$ are the Cartesian coordinates along the horizontal surface and normal to it, respectively. The velocity components are $\bar{u}$ along and $\bar{v}$ normal to the wall surface. The acceleration due to gravity g acts vertically downward. The Darcy law for a power-law fluid, given by Bird et al. [13], is

Received 17 June 2010; revision received 14 August 2010; accepted for publication 16 August 2010.

*Pakistan Navy Engineering College, Department of Engineering Sciences, PNS Jauhar, Karachi.
†Department of Mechanical Engineering.

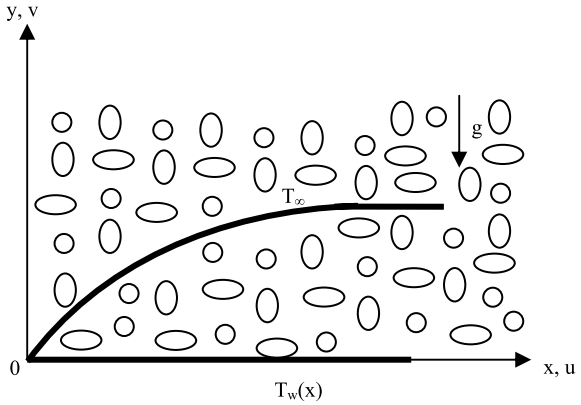

Fig. 1 Flow model and coordinate system.

$$u = -\left(\frac{K}{\mu}\cdot\frac{\mathrm{d}p}{\mathrm{d}x}\right)^{1/n}$$

or

$$u^n = -\frac{K}{\mu}\cdot\frac{\mathrm{d}p}{\mathrm{d}x}$$

But, a balance of forces gives

$$\frac{\partial p}{\partial y} = -\rho g$$

which gives

$$p = -\int \rho g \,\mathrm{d}y$$

Therefore,

$$\frac{\partial p}{\partial x} = -\frac{\partial}{\partial x}\int \rho g \,\mathrm{d}y$$

Using the Boussinesq approximation,

$$\rho = \rho_\infty[1 - \beta(T - T_\infty)]$$

we get

$$\frac{\partial}{\partial y}(u^n) = -\frac{K\rho g\beta}{\mu}\frac{\partial T}{\partial x}$$

Thus, the governing equations in dimensional form, for this case, can be written as

$$\frac{\partial \bar{u}}{\partial \bar{x}} + \frac{\partial \bar{v}}{\partial \bar{y}} = 0 \tag{1}$$

$$\frac{\partial \bar{u}^n}{\partial y} = -\frac{K\rho g\beta}{\mu}\frac{\partial \bar{T}}{\partial \bar{x}} \tag{2}$$

$$\bar{u}\frac{\partial \bar{T}}{\partial \bar{x}} + \bar{v}\frac{\partial \bar{T}}{\partial \bar{y}} = \alpha\frac{\partial^2 \bar{T}}{\partial \bar{y}^2} \tag{3}$$

with boundary conditions

$$\bar{y} = 0\text{: } \bar{v} = 0, \qquad \bar{T} = \bar{T}_\infty + A\bar{x}^\lambda \tag{4}$$

$$\bar{y} \to \infty\text{: } \bar{u} \to \bar{U}_\infty, \qquad \bar{T} \to \bar{T}_\infty \tag{5}$$

where the bars denote dimensional quantities. Using the following nondimensional variables,

$$x = \frac{\bar{x}}{L}, \qquad y = \frac{\bar{y}Pe^{1/3}}{L}, \qquad u = \frac{\bar{u}L}{\alpha Pe^{2/3}}$$
$$v = \frac{\bar{v}L}{\alpha Pe^{1/3}}, \qquad T = \frac{\bar{T} - \bar{T}_\infty}{\bar{T}_r - \bar{T}_\infty} \tag{6}$$

where Pe is the Peclet number, which determines the relative importance between convection and diffusion, defined by

$$Pe = \frac{\bar{U}_\infty L}{\alpha}$$

we get the following governing equations in dimensionless form:

$$\frac{\partial u}{\partial x} + \frac{\partial v}{\partial y} = 0 \tag{7}$$

$$\frac{\partial u^n}{\partial y} = -\gamma\frac{\partial T}{\partial x} \tag{8}$$

$$u\frac{\partial T}{\partial x} + v\frac{\partial T}{\partial y} = \frac{\partial^2 T}{\partial y^2} \tag{9}$$

with the dimensionless boundary conditions,

$$y = 0\text{: } v = 0, \qquad T = T_\infty + Ax^\lambda \tag{10}$$

$$y \to \infty\text{: } u \to U_\infty, \qquad T \to 0 \tag{11}$$

where T_∞ and U_∞ are the ambient temperature and freestream velocity, respectively. In Eq. (8), γ is the mixed convection parameter, defined by

$$\gamma = \left(\frac{L}{\alpha}\right)^{(n-1)/3}\frac{\rho K g\beta(\bar{T}_r - \bar{T}_\infty)}{\mu(\bar{U}_\infty)^{(2n+1)/3}} \tag{12}$$

Using the following transformations,

$$\eta = x^{(\lambda-n-1)/(2n+1)}y, \qquad \psi = x^{(\lambda+n+1)/(2n+1)}f(\eta)$$
$$T = T_\infty + Ax^\lambda\theta(\eta) \tag{13}$$

we get

$$u = x^{(2\lambda-1)/(2n+1)}f'(\eta)$$
$$v = -x^{(\lambda-n-1)/(2n+1)}\cdot\left\{\left(\frac{\lambda+n}{2n+1}\right)f(\eta) + \left(\frac{\lambda-n-1}{2n+1}\right)f'(\eta)\right\} \tag{14}$$

and the governing equations reduce to

$$n\cdot f'(\eta)^{n-1}\cdot f''(\eta) + \frac{\gamma(\lambda-n-1)}{2n+1}\cdot\eta\theta'(\eta) + \gamma\lambda\theta(\eta) = 0 \tag{15}$$

$$\theta''(\eta) + \left(\frac{\lambda+n}{2n+1}\right)f(\eta)\theta'(\eta) - \lambda f'(\eta)\theta(\eta) = 0 \tag{16}$$

with reduced the boundary conditions:

$$f(0) = 0, \qquad \theta(0) = 1, \qquad f'(\infty) = 1, \qquad \theta(\infty) = 0 \tag{17}$$

where primes denote the derivatives with respect to η.

Equations (15) and (16) were solved numerically for velocity and temperature profiles and gradients using an implicit finite difference method, where a step size of $\Delta\eta = 0.001$ was used in all the calculations. These gradients are used in the calculations of dimensionless entropy generation rates. It is important to note that, for $\lambda = 0$, Eqs. (15) and (16) reduce to a uniform wall temperature case.

Entropy Generation Rate

Following Bejan [6], the local rate of entropy generation in convective heat transfer from a power-law fluid can be written as

$$S_g''' = \frac{k}{T_0^2}\left[\left(\frac{\partial \bar{T}}{\partial \bar{x}}\right)^2 + \left(\frac{\partial \bar{T}}{\partial \bar{y}}\right)^2\right] + \frac{\mu}{T_0}\left(\frac{\partial \bar{u}}{\partial \bar{y}}\right)^{n+1} \tag{18}$$

where

$$\frac{\partial \bar{T}}{\partial \bar{x}} = \frac{\partial[T(\bar{T}_r - \bar{T}_\infty) + \bar{T}_\infty]}{\partial(xL)} = \left(\frac{\bar{T}_r - \bar{T}_\infty}{L}\right)\frac{\partial T}{\partial x}$$
$$\frac{\partial \bar{T}}{\partial \bar{y}} = \frac{\partial[T(\bar{T}_r - \bar{T}_\infty) + \bar{T}_\infty]}{\partial(yLPe^{-1/3})} = \frac{(\bar{T}_r - \bar{T}_\infty)Pe^{1/3}}{L}\frac{\partial T}{\partial y}$$
$$\frac{\partial \bar{u}}{\partial \bar{y}} = \frac{\partial(u\alpha Pe^{2/3}/L)}{\partial(yLPe^{-1/3})} = \left(\frac{\alpha}{L^2}\cdot Pe\right)\frac{\partial u}{\partial y} \tag{19}$$

with

$$\frac{\partial T}{\partial x} = \lambda \cdot x^{\lambda-1}\theta + x^\lambda \cdot \theta' \cdot \left(\frac{\lambda - n - 1}{2n+1}\right)\frac{\eta}{x}$$
$$= x^{\lambda-1}\left[\lambda\theta + \eta\left(\frac{\lambda - n - 1}{2n+1}\right)\theta'\right]$$
$$\frac{\partial T}{\partial y} = x^\lambda \cdot \theta' x^{(\lambda-n-1)/(2n+1)} = x^{(2\lambda-1)(n+1)/(2n+1)} \cdot \theta'$$
$$\frac{\partial u}{\partial y} = x^{(2\lambda-1)/(2n+1)} \cdot f'' \cdot x^{(\lambda-n-1)/(2n+1)} = x^{(3\lambda-n-2)/(2n+1)} \cdot f'' \tag{20}$$

Using Eqs. (19) in Eq. (18), we get the dimensionless local rate of entropy generation:

$$N_s = N_C + N_Y + N_F \tag{21}$$

where

$$N_s = \frac{S_g'''}{[k(\bar{T}_r - \bar{T}_\infty)^2/T_0^2L^2]}, \qquad N_C = \left(\frac{\partial T}{\partial x}\right)^2$$
$$N_Y = Pe^{2/3}\left(\frac{\partial T}{\partial y}\right)^2, \qquad N_F = G \cdot Pe^{n+1} \cdot \left(\frac{\partial u}{\partial y}\right)^{n+1} \tag{22}$$

with

$$G = \frac{\mu T_0 L^2}{k(\bar{T}_r - \bar{T}_\infty)^2} \cdot \left(\frac{\alpha}{L^2}\right)^{n+1} \tag{23}$$

where N_C is the entropy generation in the axial direction, N_Y is the entropy generation in the normal direction to the horizontal surface, and N_F is the entropy generation due to fluid friction.

Irreversibility Ratio

The irreversibility ratio Φ is defined by Bejan [6] as the ratio of entropy generation due to the fluid friction N_F to the total entropy generation due to heat transfer $(N_C + N_Y)$; that is,

$$\Phi = \frac{N_F}{N_C + N_Y} \tag{24}$$

It is important to note that, when $\Phi = 1$, both the heat transfer and fluid friction irreversibilities have the same contribution in generating entropy. But, when $\Phi > 1$, fluid friction dominates, and when $\Phi < 1$, heat transfer dominates.

Bejan Number

Because of the importance of the contribution of entropy generation due to heat transfer, Paoletti et al. [14] defined the Bejan number (Be) as the ratio of entropy generation due to heat transfer to the total entropy generation; that is,

$$Be = \frac{N_C + N_Y}{N_C + N_Y + N_F} = \frac{1}{1 + \Phi} \tag{25}$$

where the Bejan number ranges from 0 to 1. When the heat transfer irreversibility dominates, $Be = 1$, and when the irreversibility is dominated by fluid friction, $Be = 0$, and when the heat transfer and fluid friction entropy generation rates are equal, $Be = 1/2$.

Results and Discussion

Entropy generation rates due to heat transfer and fluid flow in the mixed convection of non-Newtonian fluids over a horizontal plate with a prescribed surface temperature are analyzed. Velocity and temperature fields are obtained by solving Eqs. (15) and (16) with boundary conditions (17), numerically using an implicit finite difference method under the similarity assumption. The effects of the temperature variation parameter λ on the dimensionless axial velocity and temperature profiles are shown in Figs. 2 and 3 for the mixed convection in both pseudoplastic and dilatant fluids. Because of the coupling of Darcy and energy equations, the velocity depends on λ, and it decreases with the increase in λ. It is observed that the

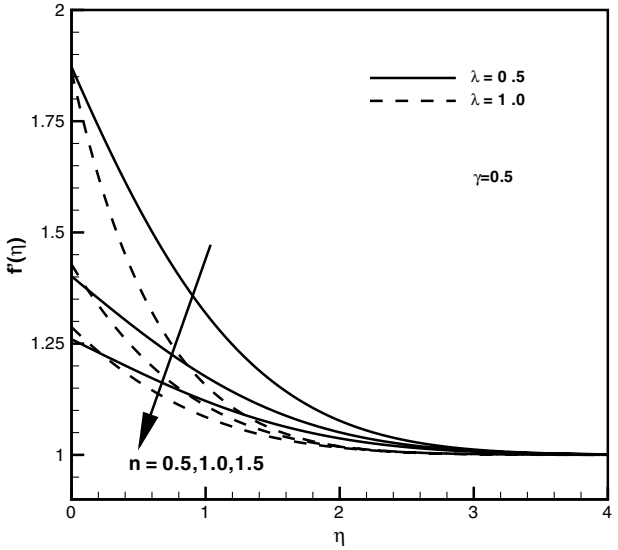

Fig. 2 Effect of λ on velocity profiles for different power-law fluids.

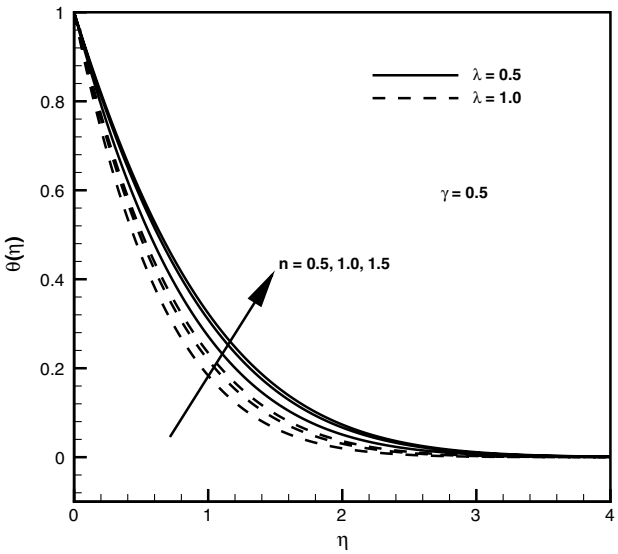

Fig. 3 Effect of λ on temperature profiles for different power-law fluids.

velocity also decreases with the increase in the flow behavior index n. The boundary-layer thickness decreases with the increase in power variation λ.

Dimensionless temperature profiles are plotted in Fig. 3 for the same values of the flow behavior index n and the temperature variation parameter λ. For the prescribed temperature boundary condition, the temperature is maximum at the wall and decreases to ambient temperature for all values of the temperature variation parameter λ and flow behavior index n. It can be observed that the effect of the flow behavior index n is less compared with that of the temperature variation parameter λ. The temperature decreases as the index n and λ increase for both pseudoplastic and dilatant fluids. An increase in the power-law index in the pseudoplastic means the non-Newtonian behavior decreases, and the fluid becomes close to Newtonian fluid, whereas an increase in the power-law index in dilatants means the non-Newtonian behavior increases and the fluid goes far from Newtonian behavior. The same behavior could be observed in Fig. 3, where the temperature profiles (for $n < 1$) are converging toward $n = 1$ and moving away for $n > 1$ (dilatant fluids).

The dimensionless entropy generation rate is plotted against the dimensionless transverse distance for different values of the temperature variation parameter for both pseudoplastic and dilatant fluids in Fig. 4. At the free surface, there is no contribution to the entropy generation rate due to zero velocity and temperature gradients. For a fixed axial distance, the magnitude of the entropy generation number is higher for the lower value of the temperature variation parameter and fluid behavior index. For both the pseudoplastic and dilatant fluids, the entropy generation rate decreases along the transverse distance to reach zero at the boundary-layer edge. This is due to the fact that, for both fluids, the velocity profile is flat near the free surface, leaving no contribution of fluid friction on entropy generation. Therefore, the entropy generation is mainly dominated by heat transfer. It is important to note that the entropy generation rate is more pronounced for pseudoplastic fluids than dilatant fluids.

The effect of the temperature variation parameter on the irreversibility ratio for pseudoplastic and dilatant fluids is shown in Figs. 5 and 6, respectively. For pseudoplastic fluids, the irreversibility ratios are found to be maximum at the boundary-layer edge, whereas for dilatant fluids, the irreversibility ratios are zero at the boundary-layer edge. These ratios decrease with the increase in the fluid behavior index n in both cases. In the case of pseudoplastic fluids, the irreversibility ratios are higher for smaller values of the temperature variation parameter, whereas in case of dilatant fluids, these ratios are higher for larger values of the temperature variation parameter.

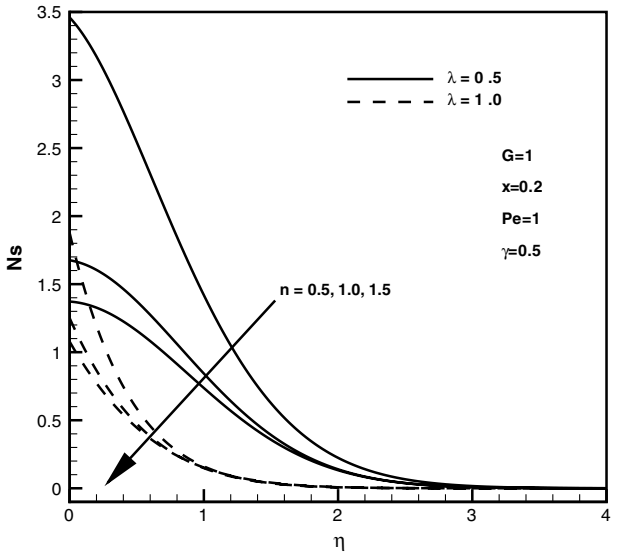

Fig. 4 Effect of λ on local dimensionless entropy generation rate for different power-law fluids.

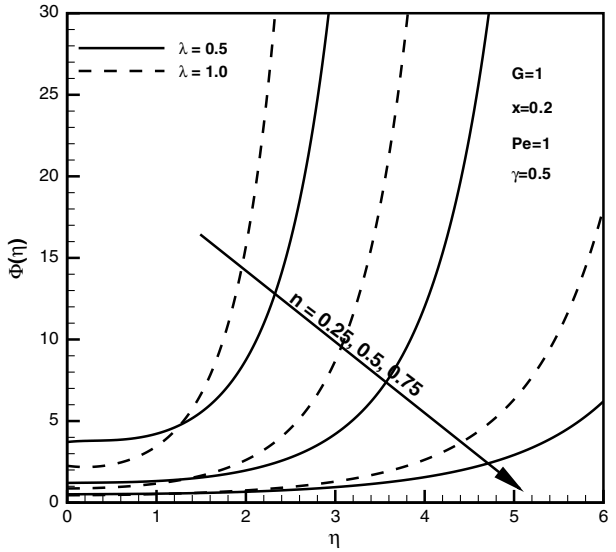

Fig. 5 Effect of λ on irreversibility ratio Φ for different pseudoplastic fluids.

The Bejan number is plotted against the dimensionless transverse distance for different values of the temperature variation parameter for both pseudoplastic and dilatant fluids in Figs. 7 and 8, respectively. It is clear from Figure 7 that the Bejan number is a decreasing function of dimensionless transverse distance, and it increases with the increase in the fluid behavior index. The Bejan number is higher at the wall surface and converges quickly due to the decrease in the boundary thickness. Dilatant fluids show the different behavior due to their nature. They increase with the dimensionless transverse distance and are maximum at the boundary-layer edge. Their values are lower at the wall surface for higher values of λ. This is shown in Fig. 8.

Figures 9 and 10 show the effect of the Pe number on the dimensionless entropy generation rate and Bejan number, respectively. It is clear that both decrease with the dimensionless transverse distance. The dimensionless entropy generation rate increases with the axial distance for both Pe numbers. Figure 9 shows that the dimensionless entropy generation rate increases with the increase in Pe numbers. Again, the dimensionless entropy generation rate is maximum at the wall surface and decreases to zero at the boundary-layer edge. The Bejan number is also found to be maximum at the wall surface and goes to zero due to no irreversibility at the boundary-layer edge. This can be observed in Fig. 10. Unlike the dimensionless

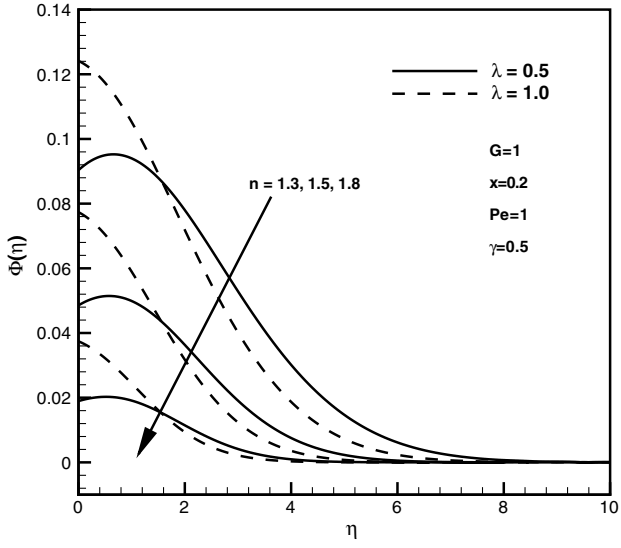

Fig. 6 Effect of λ on irreversibility ratio Φ for different dilatant fluids.

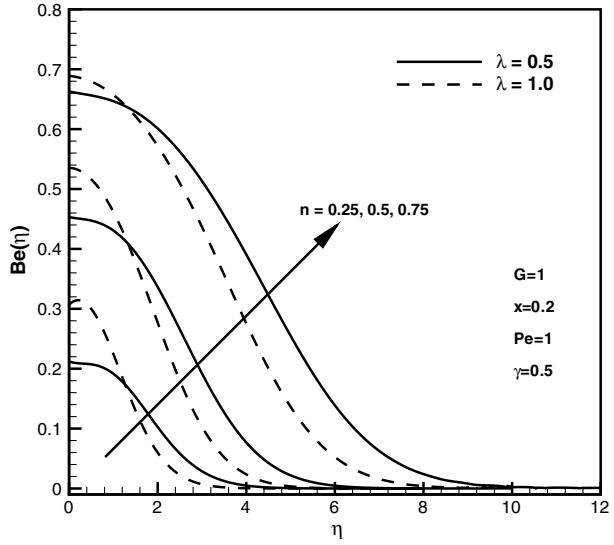

Fig. 7 Effect of λ on Bejan number *Be* for different pseudoplastic fluids.

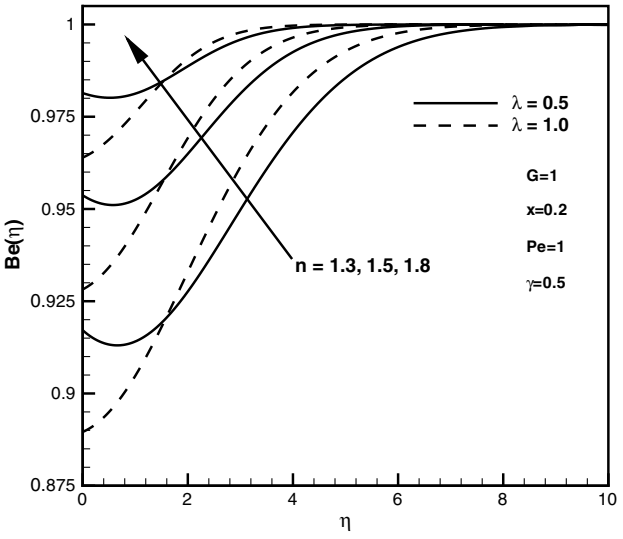

Fig. 8 Effect of λ on Bejan number *Be* for different dilatant fluids.

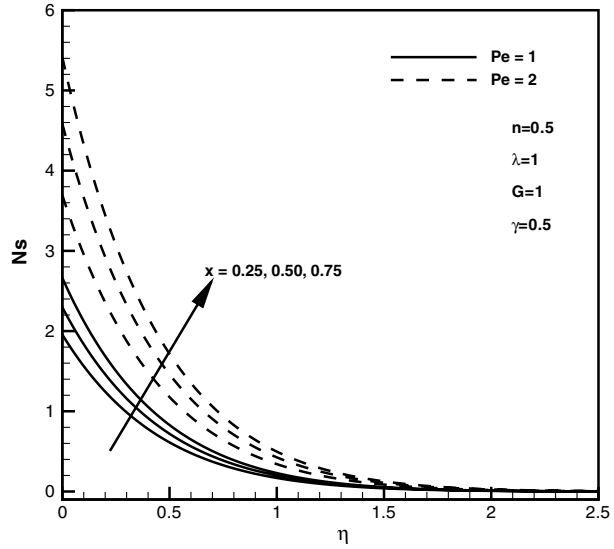

Fig. 9 Effect of *Pe* on local dimensionless entropy generation rate *Ns* for different positions in axial direction.

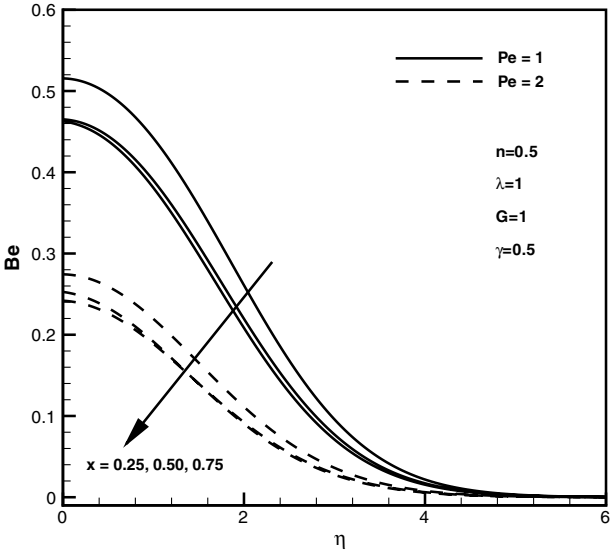

Fig. 10 Effect of *Pe* on Bejan number *Be* for different positions in axial direction.

entropy generation rate, the Bejan number decreases with the increase in the *Pe* number and the dimensionless axial distance.

Conclusions

The second-law analysis of heat transfer and fluid flow due to the mixed convection of non-Newtonian fluids over a horizontal plate is performed for the prescribed surface temperature boundary condition. The velocity and temperature fields are obtained numerically using an implicit finite difference method under the similarity assumption. It is observed that the dimensionless velocity, temperature, entropy generation rate, irreversibility ratio, and Bejan number depend upon the temperature variation parameter λ and fluid behavior index *n*. The dimensionless velocity, temperature, and entropy generation rate are found to be maximum at the wall surface and decrease to zero at the boundary-layer edge for all power-law fluids, whereas the irreversibility ratio and Bejan number go to maximum at the boundary-layer edge for pseudoplastic and dilatant fluids, respectively. The dimensionless entropy generation rate increases, whereas the Bejan number decreases with the increase in the dimensionless axial distance.

References

[1] Hossain, M. A., and Nakayama, A., "Nonsimilar Free Convection Boundary Layer in Non-Newtonian Fluid Saturated Porous Media," *Journal of Thermophysics and Heat Transfer*, Vol. 8, No. 1, 1994, pp. 107–112. doi:10.2514/3.507

[2] Hossain, M. A., and Rees, D. A. S., "Radiation-Conduction Interaction on Mixed Convection Flow Along a Slender Vertical Cylinder," *Journal of Thermophysics and Heat Transfer*, Vol. 12, No. 4, 1998, pp. 611–613. doi:10.2514/2.6387

[3] Lasode, and Olumuyiwa, A., "Perturbation Solution to Mixed Convection in Rotating Horizontal Elliptic Cylinders," *Journal of Thermophysics and Heat Transfer*, Vol. 18, No. 1, 2004, pp. 79–86. doi:10.2514/1.9154

[4] Hooper, W. B., Chen, T. S., and Armaly, B. F., "Mixed Convection along an Isothermal Vertical Cylinder in Porous Media," *Journal of Thermophysics and Heat Transfer*, Vol. 8, No. 1, 1994, pp. 92–99. doi:10.2514/3.505

[5] Ingham, D. B., and Pop, I., "Mixed Convection about a Cylinder Embedded to a Wedge in Porous Media," *Journal of Thermophysics and Heat Transfer*, Vol. 5, No. 1, 1991, pp. 117–120. doi:10.2514/3.235

[6] Bejan, A., *Entropy Generation Minimization*, CRC Press, Boca Raton, NY, 1996.

[7] Bejan, A., *Convection Heat Transfer*, Wiley, New York, 1984.

[8] Bejan, A., "A Study of Entropy Generation in Fundamental Convective

Heat Transfer," *Journal of Heat Transfer*, Vol. 101, 1979, pp. 718–725. doi:10.1115/1.3451063

[9] Saouli, S., and Aiboud-Saouli, S., "Second Law Analysis of Laminar Falling Liquid Film Along an Inclined Heated Plate," *International Communications in Heat and Mass Transfer*, Vol. 31, No. 6, 2004, pp. 879–886. doi:10.1016/S0735-1933(04)00074-0

[10] Saouli, S., and Aiboud-Saouli, S., "Second-Law Analysis of Laminar Non-Newtonian Gravity-Driven Liquid Film Along an Inclined Heated Plate with Viscous Dissipation," *Brazilian Journal of Chemical Engineering*, Vol. 26, No. 2, 2004, pp. 407–414.

[11] Gorla, R. S. R., and Pratt, D. M., "Second Law Analysis of a non-Newtonian Laminar Falling Liquid Film Along an Inclined Heated Plate," *Entropy*, Vol. 9, No. 1, 2007, pp. 30–41. doi:10.3390/e9010030

[12] Aiboud-Saouli, S., Saouli, S., Settou, N., and Meza, N., "Thermodynamic Analysis of Gravity-Driven Liquid Film Along an Inclined Heated Plate with Hydromagnetic and Viscous Dissipation Effects," *Entropy*, Vol. 8, No. 4, 2006, pp. 188–199. doi:10.3390/e8040188

[13] Bird, R. B., Stewart, W. E., and Lightfort, E. N., *Transport Phenomena*, Wiley, New York, 1960.

[14] Paoletti, S., Rispoli, F., and Sciubba, E., "Calculation of Exergetic Losses in Compact Heat Exchanger Passages," *ASME AES*, Vol. 10, American Society of Mechanical Engineers, Fairfield, NJ, 1989, pp. 21–29.